НАУЧНО-ТЕХНИЧЕСКИЙ РАЗДЕЛ

UDC 539.4

Fracture Assessment of Blunt V-Notched Graphite Specimens by Means of the Strain Energy Density

A. R. Torabi[a] and F. Berto[b,1]

[a] University of Tehran, Tehran, Iran

[b] University of Padova, Vicenza, Italy

[1] Berto@gest.unipd.it

УДК 539.4

Оценка разрушения графитовых образцов с тупым V-образным надрезом с помощью критерия плотности энергии деформации

А. Р. Тораби[а], Ф. Берто[б]

[а] Тегеранский университет, Тегеран, Иран

[б] Падуанский университет, Виченца, Италия

Проводится контроль пригодности модели хрупкого разрушения, а именно: локальной плотности энергии деформации, при прогнозировании результатов экспериментальных исследований по разрушению нормальным отрывом графитовых образцов с тупым V-образным надрезом. Рассмотрены результаты испытаний на хрупкое разрушение образцов с V-образным надрезом с разной геометрией, представленные в литературных источниках. Образцы изготовляли из однотипного крупнозернистого поликристаллического графита. Оценку разрушения проводили посредством теоретического прогнозирования разрушающей нагрузки с помощью критерия плотности энергии деформации. Параметр плотности энергии деформации вычислен путем усреднения значения локальной энергии по определенному контрольному объему, который охватывает кромку надреза. Обнаружено, что данный критерий позволяет оценивать поведение графитовых образцов с разными углами надреза и радиусами у его вершины при разрушении.

Ключевые слова: V-образный надрез, хрупкое разрушение, графит, плотность энергии деформации, нагружение нормальным отрывом.

Introduction. Graphite materials are normally utilized as heat shields in various industries like aerospace, steel making and nuclear industries etc. Such materials are vulnerable to abrupt fracture because of weak mechanical properties and high degree of brittleness. The fracture problem would be quite serious if stress

raisers such as defects, scratches, cracks and notches exist in the graphite component. The stress raisers concentrate stresses around themselves and make a hazardous region with high risk of initiating crack(s) and provoking sudden fracture. Therefore, the fracture resistance of graphite parts should be essentially investigated under mechanical loads, particularly in the presence of stress concentrators [1–5] or sharp cracks [6–8].

In general, crack problems have been more extensively investigated by the researchers than notch problems in the context of fracture mechanics, since the origin of fracture mechanics was on those components containing pre-existing cracks. A comprehensive literature review showed that crack propagation and fracture have been widely assessed by several researchers on different types of graphite materials. Under mode I loading conditions where the crack faces open with respect to each other, two main contributions were found. The first one deals with evaluating the fracture toughness of a type of nuclear graphite performed by Shi et al. [9] using a three-point bending specimen. The second investigation has been carried out by Etter et al. [10] on fracture toughness of a type of poly-crystalline graphite using a single-edge cracked beam specimen. Dealing with mixed mode fracture in graphite materials, however, more works were found in literature survey. Awaji and Sato [11] were probably the first researchers who investigated experimentally the fracture toughness of two various graphite materials by means of the cracked Brazilian disk (CBD) specimen. The fracture toughness of different graphite materials has been experimentally evaluated by Yamauchi et al. [12, 13] by means of the CBD and the semi circular bend (SCB) specimens under asymmetric three-point bending. Moreover, Li et al. [14] utilized a single-edge cracked sample to measure the mixed mode fracture toughness of a type of poly-granular graphite material. Other investigations on fracture toughness of graphite materials are also worth of mentioning (see [15–22] and references reported therein).

Nowadays, the fracture problems in which a brittle component is weakened by a notch are investigated by means of the principles of the notch fracture mechanics (NFM). Specific needs, like to connect various parts of structures and machines, force designers to introduce notches of different shapes, particularly V- and U-shaped notches, into the engineering components and structures. As mentioned above, notches concentrate stresses in the proximity of their tip making the component more prone to crack initiation. If the component is made of a brittle or quasi-brittle material (such as most of industrial graphite materials), the crack nucleates from the notch border and propagates quickly causing a sudden fracture which usually takes place immediately after a rapid crack growth. Thus, the fracture behavior of brittle components containing notches should be essentially studied by using theoretical and/or experimental methods.

Few studies have been previously carried out on the fracture of graphite materials weakened by notches. At the best of authors' knowledge, the pioneering researchers in this field were Bazaj and Cox [23] and Kawakami [24] who first investigated the notch sensitivity on different graphite materials. In the past five years, brittle fracture assessment of notched graphite components has been conducted by taking into account mainly the notch fracture mechanics approaches. Dealing with mode I loading, some recent results of research in this field have been

published in [25] where the brittle fracture in V-notched graphite components has been investigated both theoretically and experimentally. Some mode I fracture tests on three different shapes of V-notched graphite specimens, which were completely different in overall geometry, were carried out and the fracture loads were assessed by means of a stress-based fracture model named in [25] the mean stress (MS) fracture model. In [26], some experimental results were conducted on brittle fracture of V-notched Brazilian disk (V-BD) specimens made of a type of polycrystalline graphite under mixed mode loading. A stress-based brittle fracture model, namely the V-notched maximum tangential stress (V-MTS) criterion, was utilized for predicting the test results [26].

Beside the works performed in [25, 26] where commonly stress-based fracture models have been employed for the fracture assessment, the strain energy density (SED) approach, as first suggested in [27], has also been successfully used in [28–30] with the aim to assess a large bulk of static mixed mode fracture tests from various brittle and quasi-brittle materials. One of the most important advantages of the mean SED approach is the mesh independency. In fact, contrary to some parameters integrated in the local criteria (e.g., maximum principal stress, hydrostatic stress, deviatoric stress), which are mesh-dependent, the SED averaged over a control volume is substantially insensitive to the mesh refinement. As widely documented in [31, 32], refined meshes are not necessary, because the mean value of the SED on control volume can be directly determined via the nodal displacements, without involving their derivatives. As soon as the average SED is known, the notch stress intensity factors (NSIFs) can be calculated a posteriori on the basis of very simple expressions linking the local SED and the relevant NSIFs. This holds true also for the stress concentration factors (SCFs), at least when the local stress distributions ahead of the blunt notch are available for the plane problem. The extension of the SED method to three-dimensional cases is also possible as well as its extension to notched geometries exhibiting small-scale yielding.

Dealing with mixed mode I/II fracture of graphite specimens containing rounded-tip notches of various shapes, the fracture load of notches has been recently predicted successfully by using the SED model (see [33–35]).

In a more recent work, a large bulk of out-of-plane fracture tests have been conducted on laboratory-scaled V-notched graphite bars and predicted well the maximum torque that each notched bar can sustain by means of the SED criterion [36]. As a non-conventional fracture study, brittle fracture of isostatic graphite subjected to compression has been also studied experimentally by means of prismatic specimens weakened by sharp and rounded-tip V-notches [37]. The SED model has been utilized for the fracture assessment of notched graphite specimens under compressive loading, as an extension of what has been suggested in previous papers dealing with the cases of in-plane tension/shear and torsion loading in notched graphite specimens.

Some new fracture test results on U-notched graphite specimens have been reported in [38] dealing with mode I loading conditions. The specimen tested was a disc-type sample containing a central bean-shaped slit with two U-shaped ends, called U-notched Brazilian disk (UNBD). The experimental results of mode I notch fracture toughness have been assessed by means of some stress-based criteria [38].

In this research, the main target was to verify the suitability of the well-known SED criterion in predicting tensile fracture load of several blunt V-notched graphite specimens reported previously in literature [25]. The results revealed that the SED criterion could predict the experimental results very well for various notch angles and different notch tip radii.

1. **Experimental Results Reported in Literature**.

1.1. ***Material***. The material utilized in [25] for fabricating the test samples was a type of commercial coarse-grained polycrystalline graphite with the properties presented in Table 1.

T a b l e 1

Properties of the Graphite Material [25]

Material property	Value
Elastic modulus E, GPa	8.05
Poisson's ratio ν	0.2
Ultimate tensile strength σ_t, MPa	27.5
Plane-strain fracture toughness K_{Ic}, MPa$\sqrt{\text{m}}$	1.0
Bulk density (kg/m^3)	1710
Mean grain size (μm)	320
Porosity (%)	9

1.2. ***Specimen***. Three blunt V-notched specimens; completely different in overall geometry; have been utilized in [25] for mode I fracture experiments. They have been the rounded-tip V-notched three-point bend (RV-TPB), the rounded-tip V-notched semi-circular bend (RV-SCB) and the rounded-tip V-notched Brazilian disk (RV-BD) specimens [25]. Figure 1 displays such specimens schematically. The dimensions of the three test specimens are presented in Tables 2, 3, and 4.

T a b l e 2

Dimensions of the RV-TPB Specimens [25]

Specimen	ρ, mm	a, mm	L, mm	S, mm	W, mm	2α, deg
RV-TPB	1.2	10	100	60	20	30, 60, 90
	4.0	16	160	96	32	30, 60, 90

T a b l e 3

Dimensions of the RV-SCB Specimens [25]

Specimen	a, mm	D, mm	S, mm	ρ, mm	2α, deg
RV-SCB	15	60	45	1, 2, 4	30, 60, 90

T a b l e 4

Dimensions of the RV-BD Specimens [25]

Specimen	a, mm	D, mm	ρ, mm	2α, deg
RV-BD	15	60	1, 2, 4	30, 60, 90

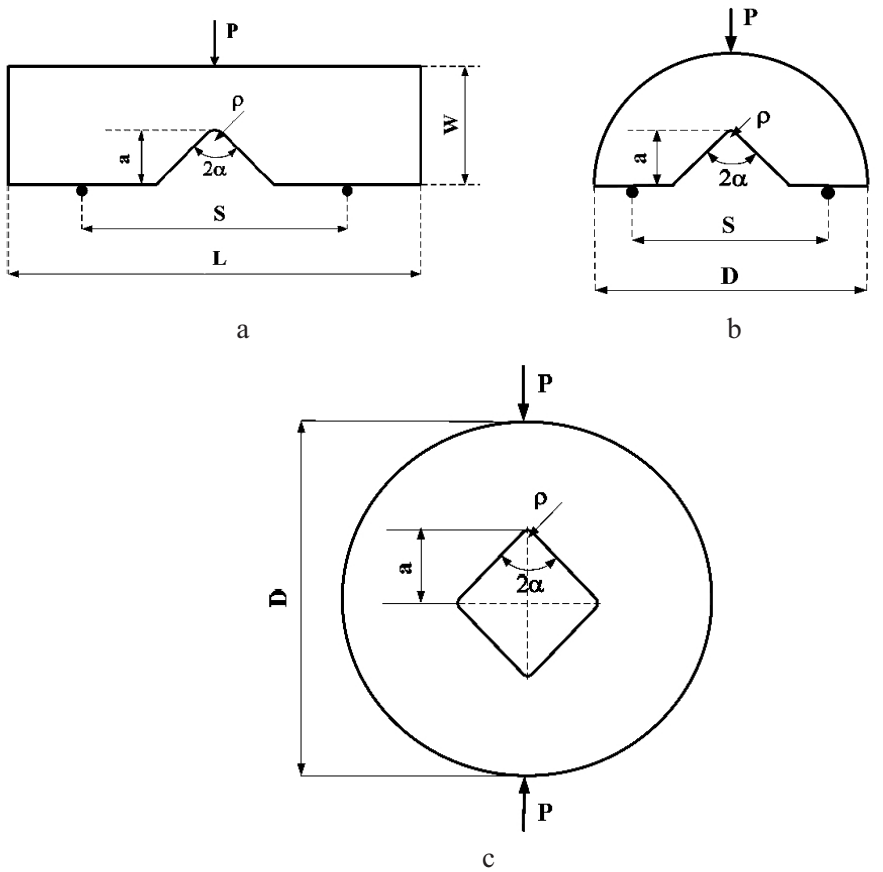

Fig. 1. The blunt V-notched test specimens used in [25] for fracture experiments: RV-TPB specimen (a), RV-SCB specimen (b), and RV-BD specimen (c).

The parameters a, ρ, and 2α denote the notch length, the notch tip radius, and the notch angle, respectively. The thickness for the entire specimens has been equal to 8 mm [25]. For each type of specimens represented in Fig. 1, three notch angles of 30, 60, and 90° and also three notch tip radii of 1, 2, and 4 mm have been considered. To check the repeatability of the experimental results, three samples have been tested for any of twenty seven geometries providing totally eighty one test results [25]. The fracture loads of the V-notched graphite specimens are presented in Table 5 [25].

Since the load–displacement curves recorded during the experiments have been linear up to final fracture [25], using the brittle fracture criteria in the context of linear elastic notch fracture mechanics (LENFM) such as the SED criterion is allowable for predicting the experimental results.

2. **Fracture Criterion Based on the Strain Energy Density Averaged Over a Control Volume**. In order to estimate the fracture load of notched graphite components, designers need a suitable fracture criterion based on the mechanical behavior of material around the notch tip. A strain-energy-density based criterion is described in this section by which the fracture loads obtained from the experiments can be estimated with a reasonable accuracy.

T a b l e 5

Fracture Loads (N) of the V-Notched Graphite Specimens [25]

Specimen	$2\alpha = 30°$			$2\alpha = 60°$			$2\alpha = 90°$		
	$\rho = 1$ (mm)	$\rho = 2$ (mm)	$\rho = 4$ (mm)	$\rho = 1$ (mm)	$\rho = 2$ (mm)	$\rho = 4$ (mm)	$\rho = 1$ (mm)	$\rho = 2$ (mm)	$\rho = 4$ (mm)
RV-TPB	153	181	261	162	196	292	162	190	305
	163	195	291	174	209	327	170	200	315
	157	189	317	170	216	345	166	212	326
RV-SCB	512	587	638	471	558	667	469	549	591
	542	633	685	490	577	726	532	572	614
	568	620	718	508	602	801	550	630	694
RV-BD	1893	1890	2057	1379	1758	1688	787	960	1110
	1939	2060	2204	1452	1574	1932	1004	1080	1250
	1875	2119	2023	1485	1606	1545	938	940	1060

Dealing with cracked components, the strain energy density factor S [39] was defined first by Sih as the product of the strain energy density by a critical distance from the point of singularity. Failure was thought of as controlled by a critical value S_c, whereas the direction of crack propagation was determined by imposing a minimum condition on S. Furthermore, this theory was used to study three problems of structural failure, namely the problem of slow stable growth of an inclined crack in a plate subjected to uniaxial tension, the problem of fracture instability of a plate with a central crack and two notches, and the problem of unstable crack growth in a circular disc subjected to two equal and opposite forces. The results of stress analysis were combined with the strain energy density theory to obtain the whole history of crack growth from initiation to instability. A length parameter was introduced to define the fracture instability of a mechanical system. Fracture trajectories were obtained for fast unstable crack propagation [40].

Different from Sih's criterion, which is a point-wise criterion, the averaged strain energy density criterion (SED) as presented in [27, 28] states that brittle failure occurs when the mean value of the strain energy density over a given control volume is equal to a critical value W_c. This critical value varies from material to material but it does not depend on the notch geometry and sharpness. The control volume, reminiscent of Neuber's concept of elementary structural volume [41], is thought of as dependent on the ultimate tensile strength and the fracture toughness $K_{\mathrm{I}c}$ in the case of brittle or quasi-brittle materials subjected to static loads.

Such a method was formalized and applied first to sharp, zero radius, V-notches under mode I and mixed I/II loading [27] and later extended to blunt U- and V-notches [28–30].

When dealing with cracks, the critical volume is a circle of radius R_c centered at the tip (Fig. 2). Under plane strain conditions, the critical length, R_c, can be evaluated according to the following expression [30]:

$$R_c = \frac{(1+\nu)(5-8\nu)}{4\pi}\left(\frac{K_{\mathrm{I}c}}{\sigma_t}\right)^2, \qquad (1)$$

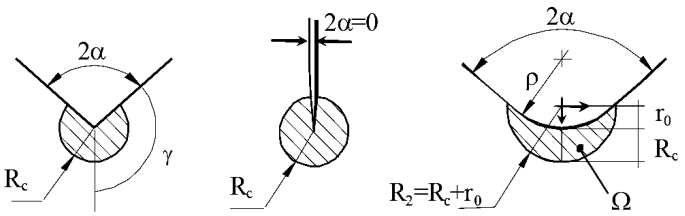

Fig. 2. Control volume (area) for sharp V-notch (a), crack (b), and blunt V-notch (c) under mode I loading. (Distance $r_0 = \rho(\pi - 2\alpha)/(2\pi - 2\alpha)$, for a U-notch $r_0 = \rho/2$.)

where K_{Ic} is the fracture toughness, ν Poisson's ratio, and σ_t the ultimate tensile strength of a plain specimen that obeys a linear elastic behavior.

For a sharp V-notch, the critical volume becomes a circular sector of radius R_c centered at the notch tip (Fig. 2) while for a blunt V-notch under mode I loading, the volume assumes the crescent shape shown in Fig. 2c, where R_c is the depth measured along the notch bisector line. The outer radius of the crescent shape is equal to $R_c + r_0$, being r_0 the distance between the notch tip and the origin of the local coordinate system (Fig. 2). Such a distance depends on the V-notch opening angle 2α, according to the expression $r_0 = \rho(\pi - 2\alpha)/(2\pi - 2\alpha)$ [28].

Under mixed mode loading, the critical volume is no longer centered on the notch tip, but rather on the point where the principal stress reaches its maximum value along the edge of the notch. It was assumed that the crescent shape volume rotates rigidly under mixed mode, with no change in shape and size. This is the governing idea of the 'equivalent local mode I' approach, as proposed and applied to U- and V-notches [29, 30].

When the area embraces the semicircular edge of the notch (and not its rectilinear flanks), the mean value of SED can be expressed in the following form [28]:

$$\overline{W}_1 = F(2\alpha)H(2\alpha, R_c/\rho)\frac{\sigma_{tip}^2}{E}, \tag{2}$$

where $F(2\alpha)$ and $H(2\alpha, R_c/\rho)$ depend on previously defined parameters and are listed in a previous reference [28]. By simply using the definition of the mode I NSIF for blunt V-notches [42], a simple relationship between σ_{tip} and $K_{1\rho}$ can be obtained as follows:

$$K_{1\rho} = \sqrt{F(2\alpha)}\,\sigma_{tip}\rho^{1-\lambda_1}. \tag{3}$$

Then, it is possible to rewrite Eq. (3) in a more compact form:

$$\overline{W}_1 = H(2\alpha, R_c/\rho)\frac{K_{1\rho}^2}{E}\frac{1}{R_c^{2(1-\lambda_1)}}. \tag{4}$$

Equation (4) can be used to evaluate the SED under mode I loading once $K_{1\rho}$ is known.

Alternatively avoiding any simplified assumption, the SED values can be directly derived from finite element (FE) models. The advantage of the direct evaluation of the SED from a FE model is that the value of this parameter is mesh-independent as described in [31, 32]. A very coarse mesh can be adopted for the SED evaluation contrary to the mesh required to evaluate the notch stress intensity factors or other stress-based parameters.

3. **SED Approach in Fracture Analysis of the Tested Graphite Specimens**. The fracture criterion described in the previous section is employed here to estimate the fracture loads obtained from the experiments conducted on the graphite specimens and taken from [25]. In order to determine the SED values, first a finite element model of the graphite specimens was generated. A typical mesh used in the numerical analyzes is shown in Fig. 3 for all the shapes of the specimens considered in the present investigation. The averaged strain energy density criterion (SED) states that failure occurs when the mean value of the strain energy density over a control volume, $\overline{W}$, is equal to a critical value W_c, which depends on the material but not on notch geometry [27, 28]. This critical value can be determined from the ultimate tensile strength σ_t according to Beltrami's expression:

$$W_c = \frac{\sigma_t^2}{2E}. \tag{5}$$

In parallel, the control volume definition via the control radius R_c needs the knowledge of the fracture toughness $K_{\mathrm{I}c}$ and Poisson's ratio ν, see Eq. (1). The critical load that is sustainable by a notched component can be estimated by imposing $\overline{W}$ equal to the critical value W_c. This value is considered here constant under mode I, mode II, and in-plane mixed-mode conditions. This assumption has been extensively verified for a number of different brittle and quasi-brittle materials [27–30].

As mentioned earlier, the properties of the graphite material used in the present investigation are: $\sigma_t = 27.5$ MPa, $K_{\mathrm{I}c} = 1$ MPa$\sqrt{\mathrm{m}}$, and Poisson's ratio $\nu = 0.2$. As a result, the critical SED for the tested graphite is $W_c = 0.0469$ MJ/m^3 whereas the radius of the control volume is $R_c = 0.429$ mm considering realistic plane strain conditions. The material properties are the same of that reported in [25, 33].

The SED occurring inside the control volume embracing the edges of V-notches has been calculated numerically by using the FE code ANSYS. For each geometry, a model was created defining the control volume where the strain energy density should be averaged (see Fig. 3). All the analyses have been carried out by using eight-node elements under the hypothesis of plane-strain conditions.

Figure 4, which refers to the case $\rho = 1$ mm and $2\alpha = 30°$, reports the strain energy density contour lines inside the control volume for the three different shapes of specimens considered herein. Note that the SED is symmetric with respect to the notch bisector line.

Tables 6–8 summarize the outlines of the experimental, numerical and theoretical findings for the tested graphite specimens with three different notch tip radii and notch opening angles investigated in the present research and re-analyzed

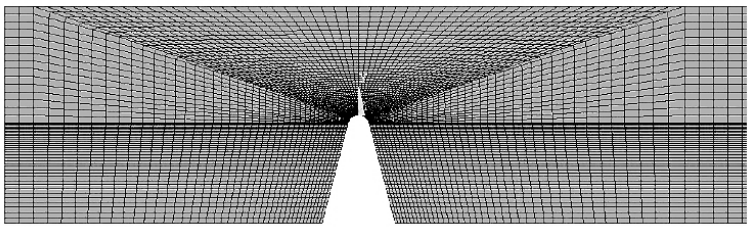

a

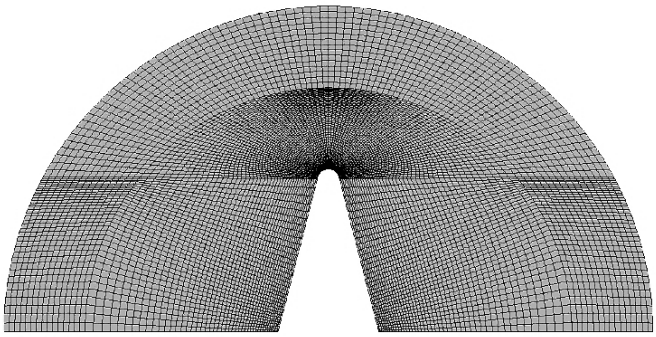

b

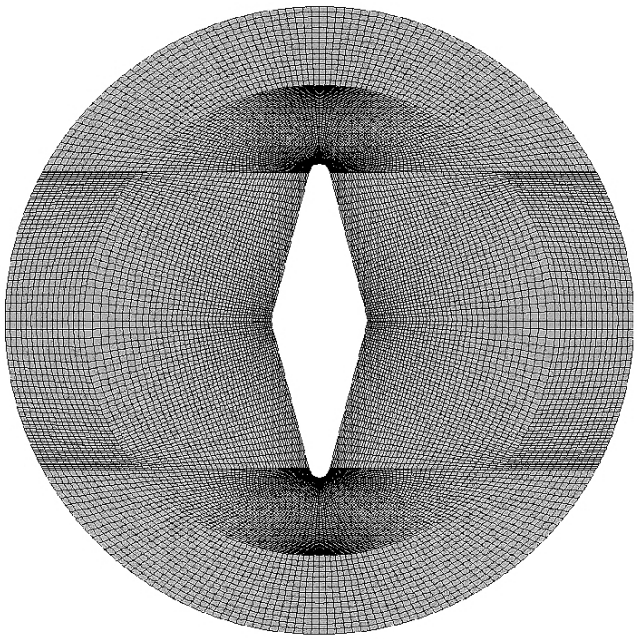

c

Fig. 3. Typical mesh used to evaluate the SED in RV-TPB (a), RV-SCB (b), and RV-BD (c) specimens.

by means of SED. In particular, each table summarizes the experimental loads to failure (P) for every notch radius ρ compared with the theoretical values (P_{th}) based on the SED evaluation. The tables also give the SED value as obtained directly from the FE models of the graphite specimens.

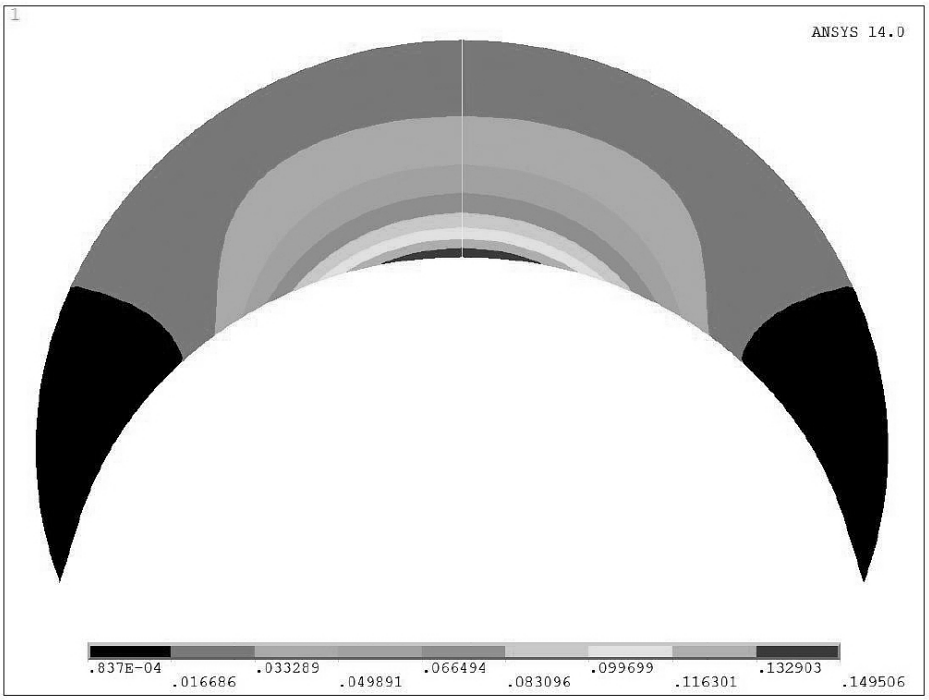

Fig. 4. SED contour lines.

T a b l e 6

Synthesis of the Results from RV-TPB Specimens

2α, deg	ρ, mm	$\overline{W}$, MJ/m^3	P, N	P_{th}, N	$\sqrt{\overline{W}/W_c}$
30	1	0.0415	153	162	0.940
		0.0470	163	162	1.001
		0.0436	157	162	0.965
	2	0.0473	181	180	1.005
		0.0549	195	180	1.082
		0.0516	189	180	1.049
	4	0.0412	261	278	0.938
		0.0512	291	278	1.045
		0.0608	317	278	1.139
60	1	0.0455	162	164	0.985
		0.0525	174	164	1.058
		0.0501	170	164	1.034
	2	0.0548	196	181	1.081
		0.0623	209	181	1.153
		0.0665	216	181	1.192
	4	0.0517	292	278	1.050
		0.0648	327	278	1.176
		0.0722	345	278	1.241

Continued Table 6

90	1	0.0446	162	166	0.976
		0.0491	170	166	1.024
		0.0468	166	166	0.999
	2	0.0514	190	181	1.047
		0.0569	200	181	1.102
		0.0640	212	181	1.168
	4	0.0563	305	278	1.096
		0.0601	315	278	1.132
		0.0643	326	278	1.172

T a b l e 7

Synthesis of the Results from RV-SCB Specimens

2α, deg	ρ, mm	$\overline{W}$, MJ/m^3	P, N	P_{th}, N	$\sqrt{\overline{W}/W_c}$
30	1	0.0615	512	447	1.145
		0.0689	542	447	1.212
		0.0757	568	447	1.270
	2	0.0636	587	504	1.165
		0.0740	633	504	1.256
		0.0710	620	504	1.231
	4	0.0546	638	591	1.079
		0.0630	685	591	1.159
		0.0692	718	591	1.215
60	1	0.0510	471	452	1.043
		0.0552	490	452	1.085
		0.0593	508	452	1.125
	2	0.0575	558	504	1.107
		0.0615	577	504	1.145
		0.0669	602	504	1.195
	4	0.0598	667	591	1.129
		0.0709	726	591	1.229
		0.0863	801	591	1.356
90	1	0.0488	469	460	1.020
		0.0628	532	460	1.157
		0.0671	550	460	1.196
	2	0.0555	549	505	1.088
		0.0602	572	505	1.133
		0.0731	630	505	1.248
	4	0.0471	591	589	1.002
		0.0508	614	589	1.041
		0.0650	694	589	1.177

T a b l e 8

Synthesis of the Results from RV-BD Specimens

2α, deg	ρ, mm	$\overline{W}$, MJ/m^3	P, N	P_{th}, N	$\sqrt{\overline{W}/W_c}$
30	1	0.0445	1893	1942	0.974
		0.0467	1939	1942	0.998
		0.0437	1875	1942	0.965
	2	0.0486	1890	1856	1.018
		0.0577	2060	1856	1.109
		0.0610	2119	1856	1.141
	4	0.0652	2057	1745	1.179
		0.0748	2204	1745	1.263
		0.0630	2023	1745	1.159
60	1	0.399	1379	1493	0.923
		0.0443	1452	1493	0.972
		0.0463	1485	1493	0.994
	2	0.0643	1758	1500	1.172
		0.0516	1574	1500	1.049
		0.0537	1606	1500	1.070
	4	0.0599	1688	1493	1.131
		0.0785	1932	1493	1.294
		0.0502	1545	1493	1.035
90	1	0.0216	787	1158	0.679
		0.0352	1004	1158	0.866
		0.0307	938	1158	0.809
	2	0.0302	960	1197	0.802
		0.0381	1080	1197	0.902
		0.0289	940	1197	0.785
	4	0.0371	1110	1247	0.889
		0.0471	1250	1247	1.002
		0.0338	1060	1247	0.849

The last column of the tables reports the square root of the SED normalized by the critical value for the material. This non-dimensional parameter is proportional to a load and quantifies the accuracy in the fracture assessment. It should be equal to 1.00 for a 0% of relative deviation between predicted and experimental values. As widely discussed in [30], acceptable engineering values range between 0.8 and 1.2. As visible from the tables, this range is satisfied for the majority of the summarized test data with only few exceptions.

Dealing with TPB specimens and notch opening angles equal to 30 and 90°, the results are given also in graphical form in Fig. 5 where the experimental values of the critical loads (open dots) have been compared with the theoretical predictions based on the constancy of the SED in the control volume (solid line). The plots are given for the notched graphite specimens as a function of the notch tip radius ρ.

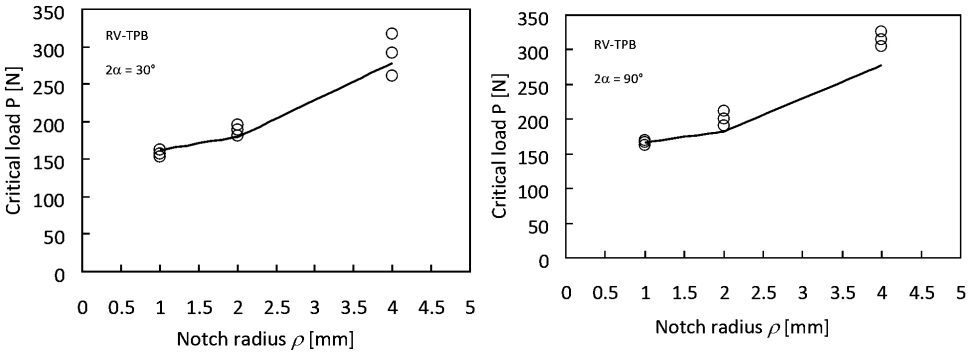

a b

Fig. 5. Comparison between theoretical fracture loads obtained by SED and experimental data for RV-TPB specimens with a notch opening angle $2\alpha = 30°$ (a) and $2\alpha = 90°$ (b).

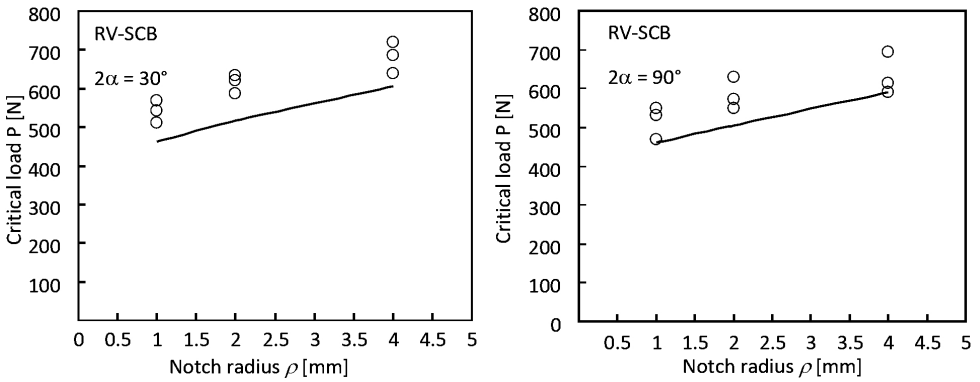

a b

Fig. 6. Comparison between theoretical fracture loads obtained by SED and experimental data for RV-SCB specimens with a notch opening angle $2\alpha = 30°$ (a) and $2\alpha = 90°$ (b).

The trend of the theoretically predicted loads is in good agreement with the experimental ones. The same comparison is shown in Fig. 6 for SCB specimens. Also in this case, it is evident that the SED is able to assess the fracture loads with a good accuracy being the predicted values also in the safe direction. Figure 7 reports the comparison between theoretical and experimental fracture loads for the BD specimens characterized by a notch opening angle $2\alpha = 60°$.

A synthesis in terms of the square root value of the local energy averaged over the control volume (of radius R_c), normalized with respect to the critical energy of the material as a function of the normalized notch tip radius is shown in Fig. 8. The plotted parameter is proportional to the fracture load. The new data are plotted together independent of the notch geometries and specimens shape. The aim is to investigate the influence of the notch tip radius on the fracture assessment based on SED. From the figure it is clear that the scatter of the data is very limited and almost independent of the notch radius. All the values fall inside a scatter ranging from 0.80 to 1.20 with the majority of the data inside 0.90 to 1.10 and only few data outside the range 0.8–1.2. The synthesis confirms also the choice of the

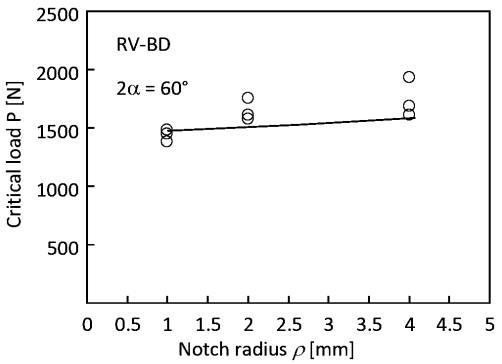

Fig. 7. Comparison between theoretical fracture loads obtained by SED and experimental data for RV-BD specimens with a notch opening angle $2\alpha = 60°$.

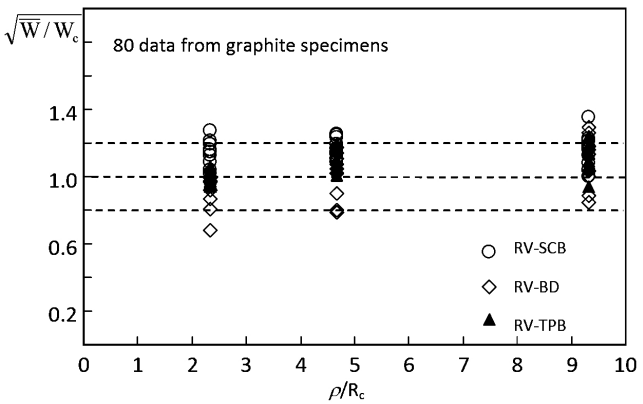

Fig. 8. Synthesis of brittle failure data from graphite specimens.

control volume which seems to be suitable to characterize the material behavior under pure mode I loading. The scatter of the experimental data presented here is in good agreement with the recent database in terms of SED reported in [29, 30].

Conclusions. The fracture loads of extensive V-notched graphite specimens reported in recent literature were theoretically predicted very well by means of the well-established brittle fracture criterion, namely the strain energy density (SED) over a specified control volume which embraces the notch edge. Three V-notched test specimens with completely various overall geometries (disk, semi-disk and rectangle) were considered in the predictions. All of the theoretical results fall inside a scatter band of $\pm 20\%$ with the majority of which inside a scatter band of $\pm 10\%$ demonstrating the effectiveness and the repeatability of the SED criterion. Only very few results fall outside the scatter band of $\pm 20\%$ that may or may not be attributed to possible inaccuracy in the experiments.

Р е з ю м е

Проводиться контроль придатності моделі крихкого руйнування, а саме: локальної густини енергії деформації, при прогнозуванні результатів експериментальних досліджень щодо руйнування нормальним відривом графітових зразків із тупим V-подібним надрізом. Розглянуто результати випробувань на

крихке руйнування зразків із V-подібним надрізом із різною геометрією, відомі з літературних джерел. Зразки виготовляли з однотипного крупнозернистого полікристалічного графіту. При оцінці руйнування використовували теоретичне прогнозування руйнівного навантаження за допомогою критерію густини енергії деформації. Параметр густини енергії деформації обчислено шляхом усереднення значення локальної енергії за визначеним контрольним об'ємом, що охоплює кромку надрізу. Установлено, що даний критерій дозволяє оцінити поведінку графітових зразків із різними кутами надрізу і радіусами у його вершині при руйнуванні.

1. M. R. Ayatollahi and S. Bagherifard, "Numerical analysis of an improved DCDC specimen for investigating mixed mode fracture in ceramic materials," *Comp. Mater. Sci*., **46**, No. 1, 180–185 (2009).
2. O. M. Herasymchuk and O. V. Kononuchenko, "Effect of surface stress concentrators and microstructure on the fatigue limit of the material," *Strength Mater.*, **43**, No. 4, 374–383 (2011).
3. V. T. Troshchenko and L. A. Khamaza, "Fatigue limits of steels and stress gradient," *Strength Mater.*, **43**, No. 4, 417–425 (2011).
4. Yu. G. Matvienko, "Approaches of fracture mechanics in the analysis of admissible defects in the form of notches," *Strength Mater*., **42**, No. 1, 58–63 (2010).
5. A. D. Pogrebnyak, M. N. Regul'skii, and A. V. Zheldubovskii, "Assessment of the effect of stress concentration on the fatigue resistance of structural materials under asymmetrical loading," *Strength Mater*., **45**, No. 1, 82–92 (2013).
6. A. Carpinteri, R. Brighenti, and S. Vantadori, "Influence of the cold-drawing process on fatigue crack growth of a V-notched round bar," I*nt. J. Fatigue*, **32**, No. 7, 1136–1145 (2010).
7. A. Carpinteri, C. Ronchei, and S. Vantadori, "Stress intensity factors and fatigue growth for surface cracks in notched shells and round bars: two decades of research work," *Fatigue Fract. Eng. Mater. Struct.*, **36**, No. 11, 1164–1177 (2013).
8. R. Brighenti and A. Carpinteri, "Surface cracks in fatigued structural components: a review," *Fatigue Fract. Eng. Mater. Struct.*, **36**, No. 12, doi: 10.1111/ffe.12100 (2013).
9. L. Shi, L. Haiyan, Z. Zhenmin, et al., "Analysis of crack propagation in nuclear graphite using three-point bending of sandwiched specimens," *J. Nucl. Mater.*, **372**, 141–151(2008).
10. T. Etter, J. Kuebler, T. Frey, et al., "Strength and fracture toughness of interpenetrating graphite/aluminum composites produced by the indirect squeeze casting process," *Mater. Sci. Eng. A*, **386**, 61–67 (2004).
11. H. Awaji and S. Sato, "Combined mode fracture toughness measurement by the disc test," *J. Eng. Mater. Tech*., **100**, 172–175 (1978).
12. Y. Yamauchi, M. Nakano, K. Kishida, and T. Okabe, "Measurement of fracture toughness for brittle materials under mixed mode impact loading

using center-notched disk specimen," *J. Soc. Mater. Sci. Jap*., **49**, No. 12, 1324–1329 (2000).

13. Y. Yamauchi, M. Nakano, K. Kishida, and T. Okabe, "Measurement of mixed-mode fracture toughness for brittle materials using edge-notched half-disk specimen," *J. Soc. Mater. Sci. Jap*., **50**, No. 3, 224–229 (2001).
14. M. Li, M. Tsujimura, and M. Sakai, "Crack-face grain interlocking/ bridging of a polycrystalline graphite: The role in mixed mode fracture," *Carbon*, **37**, No. 10, 1633–1639 (1999).
15. M. R. Ayatollahi and M. R. M. Aliha, "Mixed mode fracture analysis of polycrystalline graphite – A modified MTS criterion," *Carbon*, **46**, No. 10, 1302–1308 (2008).
16. M. Mostafavi and T. J. Marrow, "In situ observation of crack nuclei in poly-granular graphite under ring-on-ring equi-biaxial and flexural loading," *Eng. Fract. Mech*., **78**, No. 8, 1756–1770 (2011).
17. M. Mostafavi and T. J. Marrow, "Quantitative in situ study of short crack propagation in polygranular graphite by digital image correlation," *Fatigue Fract. Eng. Mater. Struct.*, **35**, No. 8, 695–707 (2012).
18. M. Mostafavi, S. A. McDonald, P. M. Mummery, and T. J. Marrow, "Observation and quantification of three-dimensional crack propagation in polygranular graphite," *Eng. Fract. Mech*., **110**, 410–420 (2013).
19. M. Mostafavi, S. A. McDonald, H. Cetinela, et al., "Flexural strength and defect behaviour of polygranular graphite under different states of stress," *Carbon*, **59**, 325–336 (2013).
20. M. Mostafavi, N. Baimpas, E. Tarleton, et al., "Three-dimensional crack observation, quantification and simulation in a quasi-brittle material," *Acta Mater.*, **61**, No. 16, 6276–6289 (2013).
21. S. Nakhodchi, D. J. Smith, and P. E. J. Flewitt, "The formation of fracture process zones in polygranular graphite as a precursor to fracture," *J. Mater. Sci.*, **48**, 720–732 (2013).
22. G. Seisson, D. Hebert, I. Bertron, et al., "Dynamic cratering of graphite: Experimental results and simulations," *Int. J. Impact Eng.*, **63**, 18–28 (2013).
23. D. K. Bazaj and E. E. Cox, "Stress concentration factors and notch sensitivity of graphite," *Carbon*, **7**, No. 6, 689–697 (1969).
24. H. Kawakami, "Notch sensitivity of graphite materials for VHTR," *J. Atom. Energ. Soc. Jap.*, **27**, No. 4, 357–364 (1985).
25. M. R. Ayatollahi and A. R. Torabi, "Tensile fracture in notched poly-crystalline graphite specimens," *Carbon*, **48**, No. 8, 2255–2265 (2010).
26. M. R. Ayatollahi and A. R. Torabi, "Failure assessment of notched poly-crystalline graphite under tensile-shear loading," *Mater. Sci. Eng. A*, **528**, No. 18, 5685–5695 (2011).
27. P. Lazzarin and R. Zambardi, "A finite-volume-energy based approach to predict the static and fatigue behavior of components with sharp V-shaped notches," *Int. J. Fract.*, **112**, No. 3, 275–298 (2001).

28. P. Lazzarin and F. Berto, "Some expressions for the strain energy in a finite volume surrounding the root of blunt V-notches," *Int. J. Fract*., **135**, No. 1-4, 161–185 (2005).
29. F. J. Gomez, M. Elices, F. Berto, and P. Lazzarin, "Local strain energy to assess the static failure of U-notches in plates under mixed mode loading," *Int. J. Fract.*, **145**, No. 1, 29–45 (2007).
30. F. Berto and P. Lazzarin, "Recent developments in brittle and quasi-brittle failure assessment of engineering materials by means of local approaches," *Mater. Sci. Eng. R* (2013). Accepted manuscript.
31. P. Lazzarin, F. Berto, F. J. Gomez, and M. Zappalorto, "Some advantages derived from the use of the strain energy density over a control volume in fatigue strength assessments of welded joints," *Int. J. Fatigue*, **30**, No. 8, 1345–1357 (2008).
32. P. Lazzarin, F. Berto, and M. Zappalorto, "Rapid calculations of notch stress intensity factors based on averaged strain energy density from coarse meshes: Theoretical bases and applications," *Int. J. Fatigue*, **32**, No. 10, 1559–1567 (2010).
33. M. R. Ayatollahi, F. Berto, and P. Lazzarin, "Mixed mode brittle fracture of sharp and blunt V-notches in polycrystalline graphite," *Carbon*, **49**, No. 7, 2465–2474 (2011).
34. F. Berto, P. Lazzarin, and C. Marangon, "Brittle fracture of U-notched graphite plates under mixed mode loading," *Mater. Design*, **41**, 421–432 (2012).
35. P. Lazzarin, F. Berto, and M. R. Ayatollahi, "Brittle failure of inclined key-hole notches in isostatic graphite under in-plane mixed mode loading," *Fatigue Fract. Eng. Mater. Struct.*, **36**, No. 9, 942–955 (2013).
36. F. Berto, P. Lazzarin, and M. R. Ayatollahi, "Brittle fracture of sharp and blunt V-notches in isostatic graphite under torsion loading," *Carbon*, **50**, No. 5, 1942–1952 (2012).
37. F. Berto, P. Lazzarin, and M. R. Ayatollahi, "Brittle fracture of sharp and blunt V-notches in isostatic graphite under pure compression loading," *Carbon*, **63**, 101–116 (2013).
38. A. R. Torabi, M. Fakoor, and E. Pirhadi, "Tensile fracture in coarse-grained polycrystalline graphite weakened by a U-shaped notch," *Eng. Fract. Mech.*, **111**, 77–85 (2013).
39. G. C. Sih, "Strain-energy-density factor applied to mixed mode crack problems," *Int. J. Fract.*, **10**, No. 3, 305–321 (1974).
40. E. E. Gdoutos, "Crack growth instability studied by the strain energy density theory," *Arch. Appl. Mech*., **82**, No. 10-11, 1361–1376 (2012).
41. H. Neuber, *Kerbspannungslehre*, 2nd edition, Springer-Verlag, Berlin (1958).
42. P. Lazzarin and S. Filippi, "A generalised stress intensity factor to be applied to rounded V-shaped notches," *Int. J. Solids Struct*., **43**, No. 9, 2461–2478 (2006).

Received 03. 09. 2013